The Nucleus **60**, No. 2 (2023) 168-173

https://doi.org/10.71330/thenucleus.2023.1296

www.thenucleuspak.org.pk

The Nucleus

ISSN 0029-5698 (Print)

ISSN 2306-6539 (Online)

Hydrothermal Synthesis and Structural Characterization of $BaTiO_3$ Powder

Muhammad Farhan Mehmood[1,2*], Amir Habib[1,3]

[1]*Department of Materials Engineering, School of Chemical and Materials Engineering (SCME), National University of Sciences and Technology (NUST), Islamabad, Pakistan*

[2]*Department for Nanostructured Materials, Jožef Stefan Institute, Jamova cesta 39, SI-1000 Ljubljana, Slovenia*

[3]*Physics Department, University of Hafar al Batin, Hafar al Batin-39524, Saudi Arabia*

ABSTRACT

The main purpose of the present study was to synthesize and characterize the structural morphology of barium titanate ($BaTiO_3$) powder. The synthesis of $BaTiO_3$ powder was carried out by hydrothermal process using barium hydroxide ($Ba(OH)_2$) and titanium dioxide (TiO_2) as precursors in a high-pressure stirred reactor autoclave for a 7-hour reaction time at various temperatures (100, 150 and 180 °C). The physical appearance of the synthesized $BaTiO_3$ powder was white crystalline. X-ray diffraction (XRD), Raman spectroscopy, and scanning electron microscopy (SEM) were used to characterize the $BaTiO_3$ powder. Raman spectroscopy and XRD techniques confirm the formation of cubic-phase $BaTiO_3$. Raman peaks at 305 and 516 cm^{-1} confirmed the formation of $BaTiO_3$. SEM micrographs showed different shapes and a highly dispersed size distribution of particles. The crystal structure of $BaTiO_3$ powder changed as the reaction temperature changed during the synthesis process. The morphological properties of the $BaTiO_3$ powder prepared at 100 °C clearly indicated spherical, irregular, and cubic rod-like structures. The particle size of $BaTiO_3$ powder was very fine at higher reaction temperatures of 150 and 180 °C. Cubic-phase $BaTiO_3$ was obtained in all the synthesized samples. Barium carbonate ($BaCO_3$) and residual unreacted TiO_2 phases as impurities were detected in the $BaTiO_3$ powder. The purity of $BaTiO_3$ powder was high at 180 °C under these synthesis conditions.

Keywords: *Cubic Phase, Powder, Hydrothermal Synthesis, X-ray Diffraction, Raman Spectroscopy, Scanning Electron Microscopy*

1. Introduction

Barium titanate ($BaTiO_3$) is the most widely used perovskite structure ceramic material due to its excellent dielectric, piezoelectric, pyroelectric, and ferroelectric properties. It has commercial applications in piezoelectric and optoelectronic devices, pyroelectric sensors, lasers, nonlinear optical devices, image processing, pattern recognition, dielectric amplifiers, and manufacturing of multilayer ceramic capacitors (MLCs) due to the high dielectric constant and low dielectric loss [1-3]. $BaTiO_3$ nanoparticles showed antibacterial activity [4] and therapeutic applications such as cancer therapy and drug delivery due to their biocompatibility [5-9]. The demand of non-conducting dielectric ceramic materials is increasing continuously and attempts are being made to reduce the size of communication devices as much as possible. Barium titanate ($BaTiO_3$) has become more and more important in ceramic materials due to its high dielectric constant and photocatalytic characteristics.

For the synthesis of high-purity $BaTiO_3$ powder, various chemical methods were used, such as barium tetanyl oxalate [10, 11] hydrolysis of barium titanium alkoxide [12, 13], co-precipitation [14-16], one-step sol-gel [17-19], molten salt [20] and hydrothermal process [21-26]. Hydrothermal synthesis process proceeds in a strong alkaline solution to prepare high-purity homogeneous and ultrafine $BaTiO_3$ powder at low-temperature (60-180 °C) chemical reactions. This process involves the chemical reaction of barium hydroxide ($Ba(OH)_2$) or barium chloride ($BaCl_2 \cdot 2H_2O$), or barium acetate ($C_4H_6BaO_4$) as barium (Ba) source and titanium dioxide (TiO_2), titanium tetrachloride ($TiCl_4$) or titanium alkoxide ($C_{12}H_{28}O_4Ti$) as titanium (Ti) source at 85-250 °C during a couple of hours reaction time. The reaction temperature has a pronounced effect on the synthesis of $BaTiO_3$ [27-30]. The formation of $BaTiO_3$ at room temperature was not experimentally observed even after 12 12-hour reaction time due to slow kinetics. $BaTiO_3$ (pseudo-cubic phase) was produced at 60 ºC and above with a small amount of $BaCO_3$ as the secondary phase [31]. This method has been widely used for the synthesis of $BaTiO_3$ powders, nanotabulars, and nanowires. The formation of cubic or tetragonal phase $BaTiO_3$ depends on temperature, the presence of counter-anions, and the characteristics of powders (size of crystallites and presence of defects) [32]. The present study is focused on synthesizing nanosized $BaTiO_3$ powder using a hydrothermal process in a stirred reactor autoclave at various reaction temperatures.

2. Experimental

Titanium dioxide powder (TiO_2; >99.90%, Merck) and barium hydroxide octahydrate ($Ba(OH)_2 \cdot 8H_2O$; 98%; Sigma-Aldrich) were used for the synthesis of $BaTiO_3$ nanopowder. Formic acid (HCOOH; 85%; Merck) was used to wash the synthesized $BaTiO_3$ powder. All the chemicals were reagent-grade and used without further purification.

For hydrothermal synthesis of $BaTiO_3$ powder, a weight of 19.0 g $Ba(OH)_2 \cdot 8H_2O$ and 3.40 g TiO_2 powder were mixed in a 250-mL Teflon reaction vessel containing 60 mL deionized water. The Teflon reaction vessel was kept in a laboratory high-pressure stirred autoclave (Model limbo li, Büchi AG, Switzerland) to operate at 100, 150 and 180 °C for 7 hours with a stirring speed of 60 rpm. After the hydrothermal reaction, the contents of the Teflon vessel were cooled to room temperature and the soluble impurities and adsorbed ions were removed with a dilute (0.25 M) formic acid solution (9.50 mL of 85% formic acid in 250 ml deionized water). The

*Corresponding author: mehmood.mfarhan@gmail.com

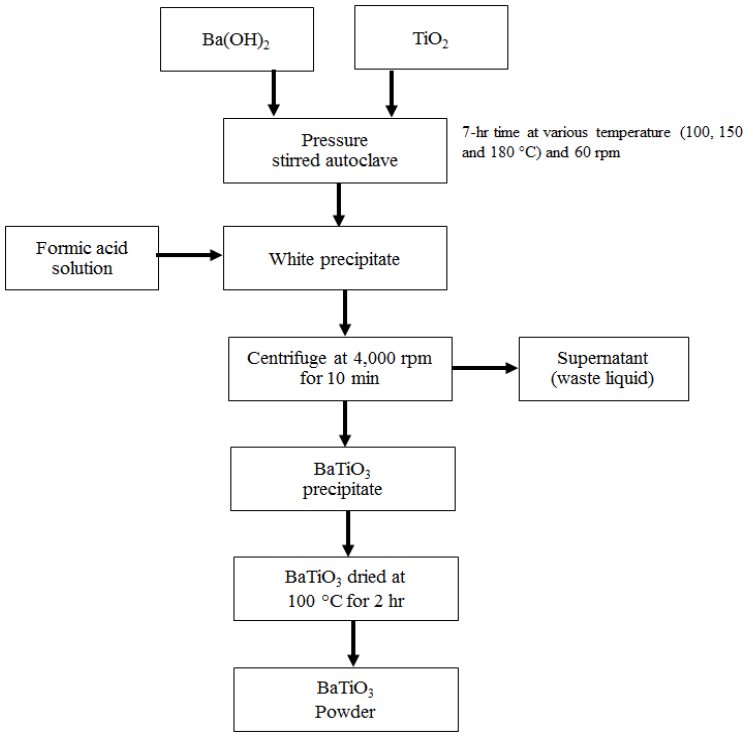

Fig. 1: Flow chart of the step-wise procedure for the synthesis of BaTiO3 powder by hydrothermal process

contents of the Teflon reaction vessel were transferred into centrifuge bottles to separate the $BaTiO_3$ precipitate. After centrifugation at 4,000 rpm for 10 min, the supernatant was decanted and the yellowish-white precipitate was washed initially with a dilute formic acid solution and then with deionized water. Finally, the washed precipitate and residue were dried in an oven at 100 °C for 2 hours.

The structural properties of the $BaTiO_3$ powder samples were characterized by X-ray diffraction (Bruker D8 Advance X-ray Diffractometer, Germany). A scanning electron microscope (Model JEOL JSM-6490A, Japan) was used to characterize the microstructure and particle morphology of $BaTiO_3$ powders. The powder samples were mounted on Cu stubs and sputter-coated with Au for 90 s using JFC-1500 ion sputtering device operated at an accelerating voltage of 20 kV. The Raman spectra of $BaTiO_3$ powders were recorded using a Micro Raman Spectrophotometer (Dongwoo Optron Co., Ltd. Korea) with a laser (532 nm) power of 150 mW equipped with a CCD detector and monochromator M320. The flow chart of the hydrothermal process of $BaTiO_3$ powder is shown in Fig. 1.

3. Results and Discussion

3.1 Synthesis of $BaTiO_3$ powders

Barium titanate ($BaTiO_3$) powders were prepared using a stirred-reactor autoclave using 19.0 g $Ba(OH)_2{\cdot}8H_2O$ and 3.40 g TiO_2 powder as precursors in 250-ml Teflon reaction vessel containing 60-ml deionized water at 100, 150, and 180 °C for 7-hour reaction time by the hydrothermal method according to the following chemical reactions:

$$Ba(OH)_2 \leftrightarrows Ba^{2+} + 2OH^- \quad (1)$$

$$TiO_2{\cdot}nH_2O + 2OH^- \leftrightarrows Ti(OH)_6^{2-} + (n\text{-}2)H_2O \quad (2)$$

$$Ba^{2+} + Ti(OH)_6^{2-} \leftrightarrows BaTiO_3 + 3H_2O \quad (3)$$

According to the above chemical reaction equilibrium, an increase in OH^- and Ba^{2+} ion concentration resulted in the formation of $BaTiO_3$ products (equations 2 and 3). An increase in the Ba-to-Ti ratio as precursors during the synthesis process resulted in the formation of $BaTiO_3$. So, the overall net chemical reaction for $BaTiO_3$ synthesis is described below:

$$Ba(OH)_2 + TiO_2 \rightarrow BaTiO_3\,(\text{crystallite}) + H_2O \quad (4)$$

The formation of $BaTiO_3$ (equation 4) is controlled by the solubility of $Ba(OH)_2$. If the limit of solubility of $Ba(OH)_2$ is reached before completion, the reaction stops and the yield is stabilized [33]. The hydrothermal process involves a simple chemical reaction between $Ba(OH)_2$ and TiO_2 in an aqueous solution in a stirred autoclave to produce $BaTiO_3$ precipitate and water. The kinetics of $BaTiO_3$ formation from $Ba(OH)_2$ and TiO_2 were studied by Hertl [30], reporting that Ba^{2+} or $Ba(OH)^+$ ions react chemically with titanium precursors to form $BaTiO_3$ by heterogeneous nucleation on its surface. The hydroxide ions (OH^{-1}) play a vital role in the nucleation of $BaTiO_3$ crystals and act as a catalyst by promoting the growth of $BaTiO_3$ under hydrothermal conditions [34]. The dynamic nature of the interaction between TiO_2, Ba^{2+}, and OH^{-1} leads to a crystallization mechanism involving nucleation, growth, and crystal dissolution. The role of OH^{-1} could be to facilitate the hydrolysis of Ti-O-Ti bonds [35].

3.2 *Characterization of $BaTiO_3$ powder*

The typical XRD patterns of the $BaTiO_3$ powders synthesized at 100, 150, and 180 °C are shown in Fig. 2. The XRD patterns of $BaTiO_3$ powders exhibited that X-ray diffraction peak intensities at 2Θ = 22.00° (100), 31.35° (110), 38.65° (111), 44.95° (200) and 55.80° (211) increased with an increase in reaction temperature during synthesis process (Fig. 2).

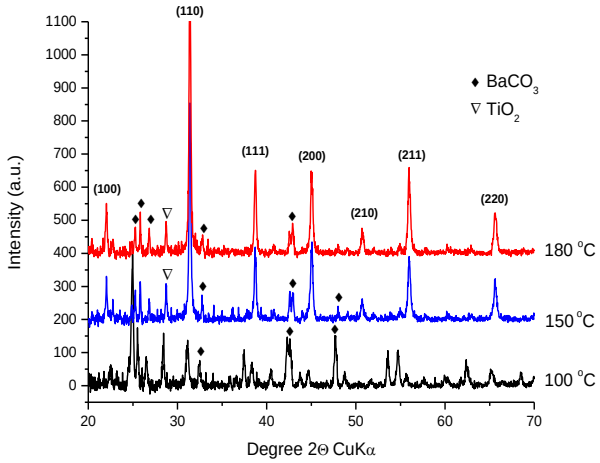

Fig. 2: XRD patterns of $BaTiO_3$ powder synthesized at 100, 150 and 180 °C by the hydrothermal process.

The unit cell parameter for the crystalline $BaTiO_3$ was determined to be a=3.994 Å and c=4.035 Å, which fit well with the peak positions of standard cubic-phase $BaTiO_3$ [JCPDS no. 01-089-1428]. It is clear that the X-ray diffraction peak (110) becomes sharper and stronger with an increase in reaction temperature. When the reaction temperature increased from 100 °C to 150 °C and then 180 °C, the XRD patterns became sharp-edged, which represents the crystallinity of $BaTiO_3$ powders. The temperatures higher than about 130 °C (Curie temperature), $BaTiO_3$ exists in the cubic perovskite structure. In this crystal structure, the Ba^{+2} ions occupy the corners of the elementary cell, the Ti^{+4} ions are in the volume center and the O^{-2} ions are in the surface center. Below the Curie point, the crystal structure transforms from the cubic phase to the distorted tetragonal structure with a displacement of the center of positive and negative charges within the sub-lattice [35]. The crystallinity of $BaTiO_3$ (cubic) was estimated by measuring the XRD intensities of cubic $BaTiO_3$ (100) peak at 2Θ = 22.160 ° with few by-products of $BaCO_3$ [36]. The XRD patterns of $BaTiO_3$ powders synthesized at 100, 150, and 180 °C clearly showed shifting of reflections around 2Θ = 45° (200) (Fig. 3). XRD patterns exhibited an appreciable increase in peak intensities and small shifting of peak positions at 150 and 180 °C that presumably due to small particle size, which confirmed the cubic structure of $BaTiO_3$ powder. The single peak reflection around 2Θ = 45° (200) region matched well with the typical XRD peaks of cubic $BaTiO_3$ [37].

The presence of $BaCO_3$ and unreacted TiO_2 phases was also identified in the products as impurities (Fig. 2). The concentration of $BaCO_3$ in the product decreased with the increase in reaction temperature (Fig. 4). Newalkar et al. [32] reported the formation of barium carbonate ($BaCO_3$)

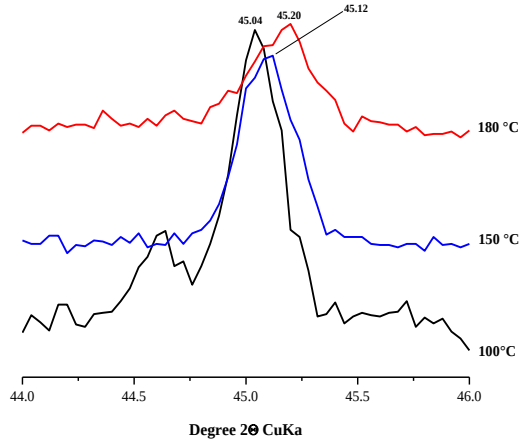

Fig. 3: XRD pattern of $BaTiO_3$ powders synthesized at 100, 150, and 180 °C showing clear reflections (200) of the cubic phase $BaTiO_3$

as a minor impurity in $BaTiO_3$ powder synthesized in the temperature range of 60-160 °C during the microwave hydrothermal process. Guo et al. [21] observed that the grain size of $BaTiO_3$ powder increased due to the agglomeration of fine particles with the increase in reaction time during the microwave hydrothermal process. $BaTiO_3$ crystallizes in the perovskite structure as a cubic lattice with barium ions occupying the corners of the unit cell, oxide ions occupying the face centers, and titanium ions occupying the centers of the unit cells. $BaTiO_3$ has a cubic structure above 120 °C.

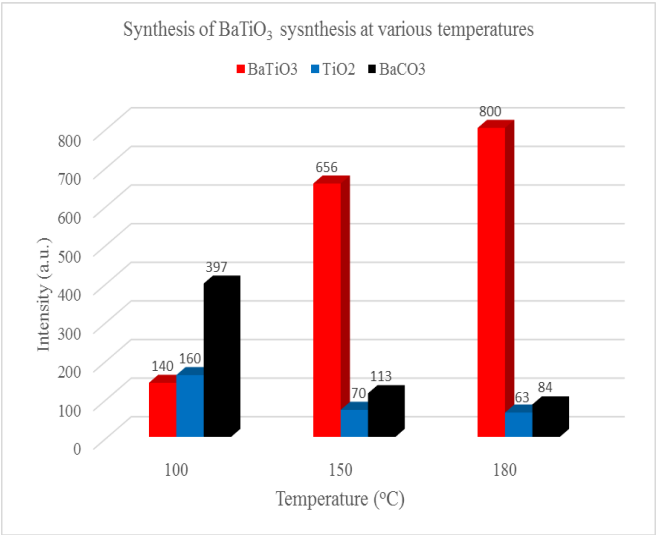

Fig. 4: XRD peak intensities show concentrations of $BaTiO_3$, $BaCO_3$, and unreacted TiO_2 in $BaTiO_3$ powders synthesized at 100, 150 and 180 °C by hydrothermal processes.

Barium carbonate ($BaCO_3$) might be decomposed to barium oxide (BaO) and carbon dioxide (CO_2) at a higher reaction temperature during the hydrothermal process and its reaction with TiO_2 could produce $BaTiO_3$, as stated by the following chemical reactions:

$$BaCO_3 \rightarrow BaO + CO_2 \quad (5)$$

$$BaO + TiO_2 \rightarrow BaTiO_3 \quad (6)$$

The decomposition reaction of $BaCO_{3\ (solid)}$ = $BaO_{\ (solid)}$ + $CO_{2\ (gas)}$ was investigated by thermogravimetric analysis (TGA) and differential thermal analysis (DTA) methods [38]. Nanocrystalline $BaTiO_3$ was prepared by solid-state reaction of TiO_2 with $BaCO_3$ of different particle sizes (650, 140, and 50 nm) [39].

The Raman scattering spectra of the $BaTiO_3$ powders synthesized at 100, 150, and 180 °C are shown in Fig. 5. The frequency range covered is from 100-1000 cm^{-1}. Raman spectra clearly showed sharp bands at 145, 160, 197, 397, 516, and 637 cm^{-1}, a sharp small band at 980 $cm^{-1,}$ and two small broad bands at 305 and 797 cm^{-1} in all the products (Fig. 5). Two broad shoulder bands at 792 and 984 cm^{-1} are also appeared in the sample obtained at 7-hour reaction time. It is clear from the Raman spectra of both samples that they contained bands of predominantly cubic-phase $BaTiO_3$ identified by the bands around 166, 196, 394, 512, and 636 cm^{-1}. It was observed that the peak intensities decreased with an increase in the reaction temperature of the synthesis process. The frequencies near 190 and 516 cm^{-1} modes come from the *F*1u cubic phase modes, the 303 cm^{-1} mode comes from the breaking of the cubic silent *F*2u mode [33]. Ávila et al. [34] suggested that the peaks at 639, 396, and 144 cm^{-1} correspond to the anatase shape of TiO_2.

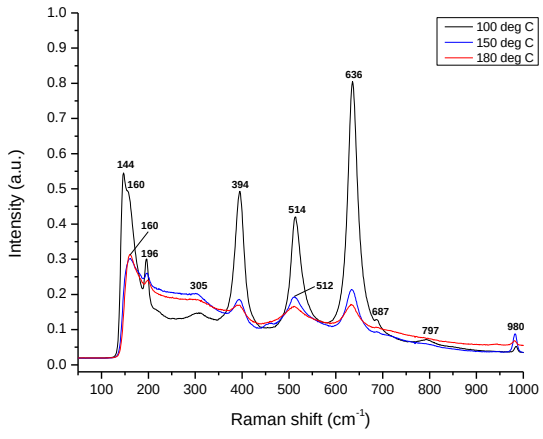

Fig. 5: Raman spectrum of $BaTiO_3$ powder prepared at 100, 150, and 180 °C by hydrothermal process. ∗ = denotes Raman peaks at 305 and 516 cm^{-1}, which correspond to $BaTiO_3$.

The experimental data shows that the chemical reaction between $Ba(OH)_2$ and TiO_2 was incomplete after 7-hour reaction time. The presence of unreacted TiO_2 coexisted in all the synthesized $BaTiO_3$ powders (Fig. 4). The concentration of unreacted TiO_2 corresponding to peak intensities decreased with an increase in reaction temperature during the synthesis process. Frey and Payne [37] suggested that the spectral peak at 193-195 cm^{-1} represents the existence of an orthorhombic $BaTiO_3$ phase. In this study, the Raman spectra showed a sharp band around 195-198 cm^{-1} in $BaTiO_3$ powders. The Raman spectra clearly showed the cubic distortion of $BaTiO_3$ structure coexisting with unreacted TiO_2 at 394 and 635 cm^{-1}. Raman bands near 630 cm^{-1} correspond to $BaCO_3$ phase, anatase TiO_2, or hexagonal $BaTiO_3$, which is stabilized at room temperature by high surface energy [40-42]. Cubic phase $BaTiO_3$ showed Raman spectrum at 166, 196, 394, 512, and 636 cm^{-1} [43]. It is clear from the Raman spectra that the synthesized powders contained bands of predominantly cubic phase $BaTiO_3$ at 166, 196, 394, 512, and 636 cm^{-1}. The intense Raman spectra near 144, 394, 514, and 636 cm^{-1} correspond to unreacted anatase TiO_2 phase in the $BaTiO_3$ powders as an impurity which is attributed to the increase of peak intensities near 394, 514, and 636 cm^{-1} due to coexistence with cubic phase $BaTiO_3$ spectral lines (Fig. 5).

SEM micrographs of $BaTiO_3$ powders are shown in Fig. 6. The $BaTiO_3$ particles showed irregular, sphere-like, cube-like particles and cube-rod structures. The average particle sizes of $BaTiO_3$ powders are 38-92, 45-63, and 28-52 nm at 100, 150, and 180 °C, respectively. The shape and particle size distribution in $BaTiO_3$ powder showed agglomeration due to nano-sized particles. $BaTiO_3$ powders synthesized at 100 °C appeared heterogeneous morphology (cube, hexagonal and rod-shaped) (Fig. 6A), whereas powder synthesized at 150 °C appeared to be very uniform spherical morphology (Fig. 6B) and cube-shaped (Fig. 6C).

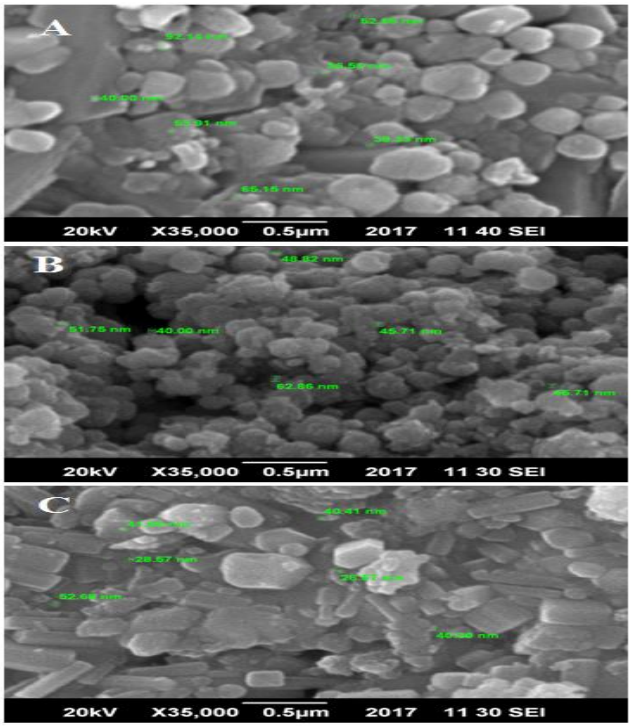

Fig. 6: SEM micrographs of $BaTiO_3$ powders synthesized at 100 °C (A), 150 °C (B), and 180 °C (C) by hydrothermal process

4. Conclusions

Hydrothermal method is the most promising route to synthesize ceramic oxide powders with controlled morphology, and high crystallinity in a one-step process. XRD and Raman spectroscopy data revealed that cubic-phase $BaTiO_3$ powders were successfully synthesized by hydrothermal processes. It is clear that cubic-phase $BaTiO_3$ nanocrystalline powder was directly crystallized by using $Ba(OH)_2{\cdot}8H_2O$ to TiO_2 at a ratio of (4:1) as a starting material in a stirred reactor autoclave by hydrothermal process. The hydrothermal synthesis process offers a promising approach to producing high-purity crystalline $BaTiO_3$ powder.

Acknowledgments

The authors are very grateful to the Department of Materials Engineering, School of Chemical and Materials Engineering (SCME), NUST, Islamabad, for assistance of scanning electron microscopy and NILOP for Raman Spectroscopy.

References

[1] Q. Feng, M. Hirasawa, K. Yanagisawa, "Synthesis of crystal-axis-oriented $BaTiO_3$ and anatase platelike particles by a hydrothermal soft chemical process," Chemistry of Materials, vol. 13, pp. 290-296, 2001.

[2] W.L. Suchanek, R.E. Rimen, "Hydrothermal synthesis of advanced ceramic powders," Advances in Science & Technology, vol. 45, pp. 184-193, 2006.

[3] M.M. Vijatović, J.D. Bobić, B.D. Stojanović, "History and challenges of barium titanate: Part II," Science of Sintering, vol. 40, pp. 235-244, 2008.

[4] A.A. Shah, A. Khan, S. Dwivedi, J. Musarrat, and A. Azam, "Antibacterial and antibiofilm activity of barium titanate nanoparticles," Materials Letters, vol. 229, pp. 30-133, 2018.

[5] M. Ahamed, M.J. Akhtar, M.A.M. Khan, H.A. Alhadlaq, and A. Alshamsan, "Barium titanate ($BaTiO_3$) nanoparticles exert cytotoxicity through oxidative stress in human lung carcinoma (A549) cells," Nanomaterials, vol. 10, Article No. 2309, 2020.

[6] T.M. Alfareed, Y. Slimani, M.A. Almessiere, M. Nawaz, F.A. Khan, A. Baykal, E.A. Al-Suhaimi, "Biocompatibility and colorectal anti-cancer activity study of nanosized $BaTiO_3$ coated spinel ferrites," Scientific Reports, vol. 12, Article No. 14127, 2022.

[7] M. Fakhar-e-Alam, S. Saddique, N. Hossain, A. Shahzad, Inaam Ullah, A. Sohail, M.J.I. Khan, and M. Saadullah, "Synthesis, characterization and application of $BaTiO_3$ nanoparticles for anti-cancer activity," Journal of Cluster Science, vol. 34, pp. 1745-1755, 2023.

[8] Y.N. Yoon, D.S. Lee, H.J. Park, and J-S. Kim, "Barium titanate nanoparticles sensitise treatment-resistant breast cancer cells to the antitumor action of tumour-treating fields," Scientific Reports, vol. 10, Article No. 2560, 2020.

[9] G.G. Genchi, A. Marino, A. Rocca, V. Mattoli, and G. Ciofani, "Barium titanate nanoparticles: promising multitasking vectors in nanomedicine," Nanotechnology, vol. 27, 232001, 2016.

[10] K. Hur, J. Lee, "Method for preparing $BaTiO_3$ powder by oxalate synthesis," United State Patent US6, 692, 721, B2, 2004.

[11] N.B. Mahmood, and E.K. Al-Shakarchi, "Three techniques used to produce $BaTiO_3$ fine powder," Journal of Modern Physics, vol. 2, pp. 1420-1428, 2011.

[12] M. Zeng, N. Uekawa, T. Kojima, and K. Kakegawa, "Formation process of $BaTiO_3$ particles by reaction between barium hydroxide aqueous solution and titania obtained by hydrolysis of titanium alkoxide," Journal of Materials Research, vol. 22, issue 8, pp. 2631-2638.

[13] T.M. Stawski, S.A. Veldhuis, R. Besselink, H.L. Castricum, G. Portale, D.H.A. Blank, and J.E. ten Elshof, "Nanostructure development in alkoxide-carboxylate-derived precursor films of barium titanate," The Journal of Physical Chemistry C, vol. 116, pp. 425-434, 2012.

[14] J.M. Hwu, W.H. Yu, W.C. Yang, Y.W. Chen, and Y.Y. Chou, "Characterization of dielectric barium titanate powders prepared by homogeneous precipitations chemical reaction for embedded capacitor applications," Materials Research Bulletin, vol. 40,issue. 10, pp. 1662-1679, 2005.

[15] M.Z.-C. Hu, G.A. Miller, E.A. Payzant, and C.J. Rawn, "Homogeneous (co)precipitation of inorganic salts for synthesis of monodispersed barium titanate particles," Journal of Materials Science, vol. 35, pp. 2927-2936.

[16] C.-J. Huang, K.-L. Chen, P.-H. Chiu, P.-W. Sze, and Y.-H. Wang, "The novel formation of barium titanate nanodendrites," Journal of Nanomaterials, vol. 2014, Article ID 718918, 6 pages, 2014.

[17] K.-M. Hung, W.-D. Yang, and C.-C. Huang, "Preparation of nanometer-sized barium titanate powders by a sol-precipitation process with surfactants," Journal of the European Society, vol. 23, issue 11, pp. 1901-1910, 2003.

[18] G. Pfaff, "Sol-gel synthesis of barium titanate powders of various compositions," Journal of Materials Chemistry, vol. 2, issue 6, pp. 591-594, 1992.

[19] A. Kareiva, S. Tautkus, and R. Rapalaviciute, "Sol-gel synthesis and characterization of barium titanate powders," Journal of Materials Science, vol. 34, pp. 4853-4857, 1999.

[20] S Ahda, S Misfadhila, P Parikin, and T.Y.S. P Putra, "Molten salt synthesis and structural characterization of $BaTiO_3$ nanocrystal ceramics," IOP Conference Series: Materials Science and Engineering, vol. 176, Article No. 012048, 2017.

[21] L. Guo, H. Luo, J. Gao, L. Guo, and J. Yang, "Microwave hydrothermal synthesis of barium titanate powders," Materials Letters, vol. 60, issue 24, pp. 3011-3014, 2006.

[22] İ.C. Kaya, V. Kalem, H. Akyildiz, "Hydrothermal synthesis of pseudocubic $BaTiO_3$ nanoparticles using TiO_2 nanofibers: Study on photocatalytic and dielectric properties," Applied Ceramic Technology, vol. 16, issue 4, pp. 1557-569, 2019.

[23] H. Chen, J. Wang, X. Yin, C. Xing, J. Li, H. Qiao, and F. Shi, "Hydrothermal synthesis of $BaTiO_3$ nanoparticles and role of PVA concentration in preparation, "Materials Research Express, vol. 6, No. 5, 055028, 2019.

[24] J. Moon, E. Suvaci, A. Morrone, S.A. Costantino, and J.H. Adair, "Formation mechanisms and morphological changes during the hydrothermal synthesis of $BaTiO_3$ particles from a chemically modified, amorphous titanium (hydrous) oxide precursor," Journal of the European Society, vol. 28, issue 12, pp. 2153-2161.

[25] S.W. Lu, B.I. Lee, Z.L. Wang, and W.D. Samuels, "Hydrothermal synthesis and structural characterization of $BaTiO_3$ nanocrystals," Journal of Crystal Growth, vol. 219, issue 3, pp. 269-276, 2000.

[26] X. Zhua, J. Zhua, S. Zhoua, Z. Liua, N. Minga, and D. Hesseb, "$BaTiO_3$ nanocrystals: Hydrothermal synthesis and structural characterization,: Journal of Crystal Growth, vol. 283, issues 3-4, pp. 553-562, 2005.

[27] S. Zhigang, Z. Weiwei, C. Jianfeng, and J. Yun, "Low temperature one step synthesis of barium titanate: Particle formation mechanism and large-scale synthesis," Chinese Journal of Chemical Engineering, vol. 14, issue 5, pp. 642-648, 2006.

[28] R. Asiaie, W. Zhu, S.A. Akbar, and P.K. Dutta, "Characterization of submicron particles of tetragonal $BaTiO_3$," Chemistry of Materials, vol. 8, issue 1, pp. 226-234, 1996.

[29] P. Pinceloup, C. Courtois, A. Leriche, and B. Thierry, "Hydrothermal synthesis of nanometer-sized barium titanate powders: Control of barium/titanium ratio, sintering, and dielectric properties," Journal of American Ceramic Society, vol. 82, issue 11, pp. 3049-3056, 1999.

[30] W. Hertl, "Kinetics of barium titanate synthesis," Journal of the American Ceramic Society, vol. 71, pp. 879-883, 1988.

[31] M.M. Lencka, and E. Riman, "Thermodynamic modeling of hydrothermal synthesis of ceramic powders," Chemistry of Materials, vol. 5, issue 1, pp. 61-70, 1993.

[32] B.L. Newalkar, S. Komarneni, and H. Katsuki, "Microwave-hydrothermal synthesis and characterization of barium titanate powders," Materials Research Bulletin, vol. 36, issue 13-14, pp. 2347-2355, 2001.

[33] Z. Lazarević, N. Romćević, M. Vijatvić, N. Paunović, M. Romćević, B. Stojanović, and Z. Dohćević-Mitrović, "Characterization of barium titanate ceramic powders by Raman spectroscopy," Acta Physica Polonica A, vol. 115, pp. 808-810, 2009.

[34] H.A. Ávila, L.A. Ramajo, M.M. Rebreed, M.S. Castro, and R. Parra, "Hydrothermal synthesis of $BaTiO_3$ from different Ti-precursors and microstructural and electrical properties of sintered samples with submicrometric grain size," Ceramics International, vol. 37, pp. 2383-2390, 2011.

[35] R. Vijayalakshmi, and V. Rajendran, "synthesis and characterization of cubic $BaTiO_3$ nanorods via facile hydrothermal method and their optical properties," Digest Journal of Nanomaterials and Biostructures, vol. 5, issue 2, pp. 511-517, 2010.

[36] P. Nanni, M. Leoni, V. Buscagalia and G. Aliprandi, Low-temperature aqueous preparation of barium metatitanate powders," Journal of the European Ceramic Society, vol. 14, issue 1, pp. 85-90, 1994.

[37] M.H. Frey, and D.A. Payne, "Grain size effect on structure and phase transformations for barium titanate," Physical Review B, vol. 54, pp. 3158-3168, 1996.

[38] I. Arvanitidis, D. Sichen, and S. Seetharaman, "A study of the thermal decomposition of $BaCO_3$," Metallurgical and Materials Transactions B, vol. 27, pp. 409-416, 1996.

[39] M.T. Buscaglia, M. Bassoli, and V. Buscaglia, "Solid-state synthesis of ultrafine $BaTiO_3$ powders from nanocrystalline $BaCO_3$ and TiO_2," Journal of American Ceramic Society, vol. 88, issue 9, pp. 2374-2379, 2005.

[40] J. Yu, and J. Chu, "Encyclopedia of Nanoscience and Nanotechnology," vol. 6, pp. 389-416, 2004.

[41] Y. Shiratori, C. Pithan, J. Dornseiffer, R. Waser, "Raman scattering studies on nanocrystalline $BaTiO_3$," part I- isolated particles and aggregates," Journal of Raman Spectroscopy, vol. 38, pp. 1288-1299, 2007.

[42] Y.X. Gan, A.H. Jayatissa, Z. Yu, X. Chen, and M. Li, "Hydrothermal synthesis of nanomaterials, "Journal of Nanomaterials,' vol. 2020, Article ID 8917013, pp. 1-3, 2020.

[43] J.L. Parson, and L.Rimai, "Raman spectrum of $BaTiO_3$," Solid State Communications, vol. 5, pp. 423-427, 1967.